CHEMISTRY
A EUROPEAN JOURNAL

DOI: 10.1002/chem.200601545

Long Synthetic Nanotubes from Calix[4]arenes

Voltaire G. Organo, Valentina Sgarlata, Farhood Firouzbakht, and Dmitry M. Rudkevich*[a]

Abstract: We report the synthesis and encapsulation properties of long (up to 5 nm) molecular nanotubes **1**–**4**, which are based on calix[4]arenes and can be filled with multiple nitrosonium (NO^+) ions upon reaction with NO_2/N_2O_4 gases. These are among the largest nanoscale molecular containers prepared to date and can entrap up to five guests. The structure and properties of tubular complexes **1**·$(NO^+)_2$–**4**·$(NO^+)_5$ were studied by UV/Vis, FTIR, and ^{1}H NMR spectroscopy in solution, and also by molecular modeling. Entrapment of NO^+ in **1**·$(NO^+)_2$–**4**·$(NO^+)_5$ is reversible, and addition of [18]crown-6 quickly recovers starting tubes **1**–**4**. The FTIR and titration data revealed enhanced binding of NO^+ in longer tubes, which may be due to cooperativity. The described nanotubes may serve as materials for storing and converting NO_x and also offer a promise to further develop supramolecular chemistry of molecular containers. These findings also open wider perspectives towards applications of synthetic nanotubes as alternatives to carbon nanotubes.

Keywords: calixarenes · molecular recognition · nanotubes · nitrogen oxides · supramolecular chemistry

Introduction

A novel type of molecular container is quickly emerging, namely, the synthetic nanotube.[1–3] In contrast to other molecular containers such as cavitands, (hemi)carcerands, and self-assembling capsules, much developed over the last decade,[4] nanotubes have different topology, are open at both ends, and therefore feature different guest dynamics upon encapsulation.

The inspiration comes from naturally occurring ion channels[5] and, on the technological side, single-walled carbon nanotubes (SWNTs).[6] The major feature of nanochannels and nanotubes is the ability to align multiple guest species in one dimension, which is important for nanowiring, molecular and ion transport, and information flow. Other potential applications include using nanotubes as reaction vessels and molecular cylinders for storage. While synthesis offers a variety of sizes and shapes, synthetic nanotubes are still rare. One reason is the significant technical difficulty associated with building defined and long nanostructures through multiple bonding. The other problem is to achieve stable encapsulation complexes and control the behavior of guests inside. Most of the synthetic nanotubes and channels known to date are formed by self-assembly and thus stable only under specific, rather mild conditions.[1,5] There have been several breakthroughs in filling SWNTs, but it is not trivial to identify and study the encapsulated species.[6]

Here we present a full report on synthesis and encapsulation properties of long synthetic nanotubes.[7] They are covalently built and robust and their length is controlled precisely and easily through modular synthesis. These nanotubes can interact with NO_x gases, convert them, and thus be easily filled. As a consequence, they form kinetically and thermodynamically stable but reversible encapsulation complexes. These complexes can be studied by conventional spectroscopic techniques. With lengths of up to 5 nm and with up to five guests entrapped, these nanotubes are the largest synthetic molecular containers known to date. Taken together, our synthetic nanotubes can serve as alternatives to SWNTs for filling purposes and further applications.

[a] Dr. V. G. Organo, Dr. V. Sgarlata, F. Firouzbakht, Prof. Dr. D. M. Rudkevich
Department of Chemistry & Biochemistry
The University of Texas at Arlington
Arlington, TX 76019-0065 (USA)
Fax: (+1) 817-272-3808
E-mail: rudkevich@uta.edu

Results and Discussion

Design and synthesis: For filling purposes, stable encapsulation complexes are needed. However, with synthetic nanotubes such stability is rarely achieved due to the lack of additional binding sites within their interiors.[1,2] The major

drawback of encapsulation complexes with gases, including those formed by SWNTs, also lies in their relatively low thermodynamic stability.[8] An alternative approach is based on reversible chemical transformation of gases upon encapsulation. In this case, they produce reactive intermediates with much higher affinities for the receptor molecules. Higher stabilities of such host–guest complexes result in better sensors and also offer attractive opportunities for the design of chemical reagents from gases, as well as conceptually novel materials for gases and from gases. This approach has been successful for NO_x. Kochi, Rathore, and co-workers showed that, when converted to the cation radicals, simple calix[4]arenes can strongly bind NO gas with formation of cationic calixarene–nitrosonium species.[9] In these, the NO molecule is transformed into nitrosonium (NO^+) cation, which is tightly encapsulated inside the calixarene cavity. We recently discovered that calix[4]arenes reversibly interact with NO_2/N_2O_4 and entrap highly reactive NO^+ cation within their π-electron-rich interiors.[10] NO^+ is generated from N_2O_4, which is known to disproportionate to NO^+ NO_3^-. Only one NO^+ ion was found per cavity; very high association constants ($K_{assoc} \geqslant 10^6\,M^{-1}$) were determined. We took advantage of this unique chemistry between calixarenes and NO_x gases for the design and filling of nanotubes **1**–**4**.

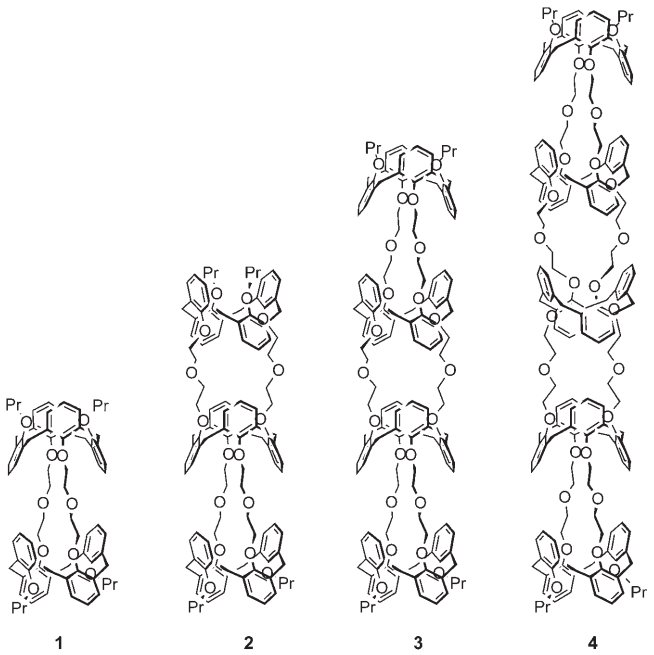

In the design of nanotubes **1**–**4**, several calix[4]arenes are rigidly connected from both sides of their rims with two symmetrical bridges. This is possible for a 1,3-alternate conformation. Calix[4]arenes in a 1,3-alternate conformation are more rigid than other conformers and have a cylindrical inner tunnel, formed by two cofacial pairs of aromatic rings oriented orthogonally along the cavity axis. According to a number of X-ray studies, this tunnel is 6 Å in diameter.[7] Two pairs of phenolic oxygen atoms, oriented in opposite directions, provide diverse routes to enhance the tube length modularly. For the connection, diethylene glycol bridges were chosen, which not only provide relatively high conformational rigidity of the tubular structure, but also seal the walls by minimizing the gaps between the calixarene modules.

The synthesis of nanotubes **2**–**4** is based on a straightforward, modular strategy which incorporates reliable Williamson-type alkylations and provides high yields (Schemes 1 and 2). Trimeric tube **2** was synthesized in 70% yield by coupling of tetratosylate **5**[11] with two equivalents of diol **6**[7b] in boiling THF with NaH as base. Tube **3**, which contains four calixarenes, was prepared by reaction of bis-calixarene diol **7** with ditosylate **8** in 64% yield (NaH, K_2CO_3, THF). Finally, reaction of two equivalents of diol **7** with tetratosylate **5** under the same conditions afforded pentameric nanotube **4** in a remarkable 82% yield. The successful use of K_2CO_3 in addition to NaH in these last cases can possibly be explained by template effects. Some calixarene–crown derivatives are known to strongly complex K^+ ion.[3a]

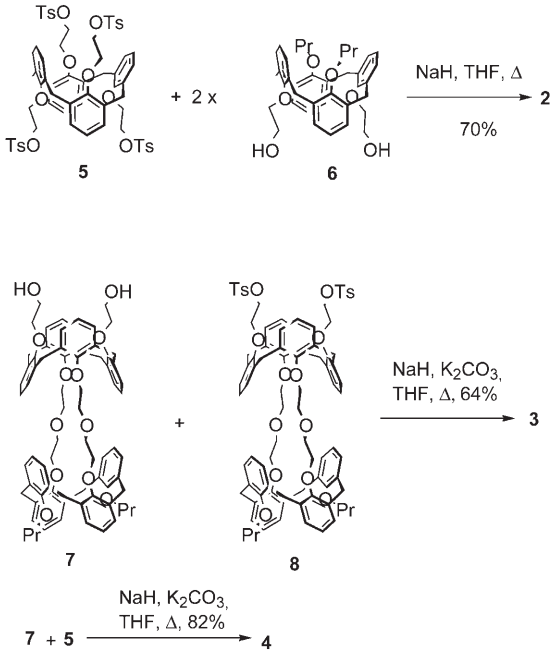

Scheme 1. Synthesis of nanotubes **2**–**4**.

Syntheses of precursors for tubes **3** and **4** are based on conventional calixarene transformations. 25,27-Bis[2-benzyloxy)ethyloxy]-26,28-dihydroxycalix[4]arene (**9**) was obtained by alkylation of the parent, commercially available calix[4]arene with 2-(benzyloxy)ethanol *p*-toluenesulfonate and K_2CO_3 in hot MeCN in 71% yield. It was further alkylated with 2-(*tert*-butyldimethylsiloxy)ethanol *p*-toluenesulfonate and Cs_2CO_3 in DMF with the formation of 1,3-alternate calixarene **10** in 67% yield. Derivative **10** was then desilylated with acetyl chloride in MeOH, and the resulting

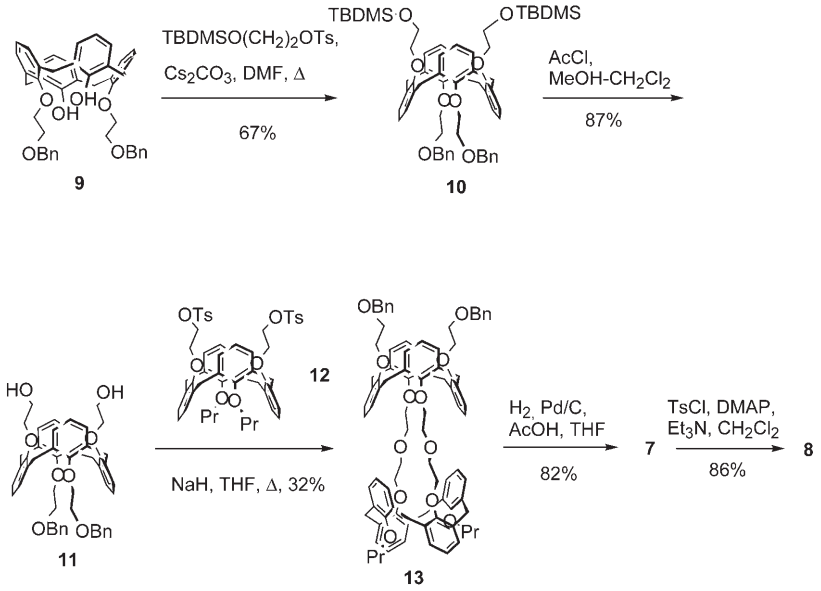

Scheme 2. Synthesis of calix[4]arene precursors **7**–**13**.

diol **11** was coupled to ditosylate **12**[12] in THF in the presence of NaH as base. This afforded tubular bis-calixarene **13** in 32% yield, which was subsequently debenzylated (H_2, Pd/C, AcOH, THF) to give **7** in 82% yield. This was smoothly (86%) converted to ditosylate **8** by using *p*-toluenesulfonyl chloride, Et_3N, and 4-dimethylaminopyridine (DMAP) in CH_2Cl_2.

Nanotubes **1**–**4** have an inner tunnel of 6 Å in diameter and are 17, 26, 35, and 45 Å long, respectively (Figure 1). Tubes **3** and **4** have molecular weights of approximately 2.3 and 2.8 kDa, which definitely qualifies them as nanostructures.

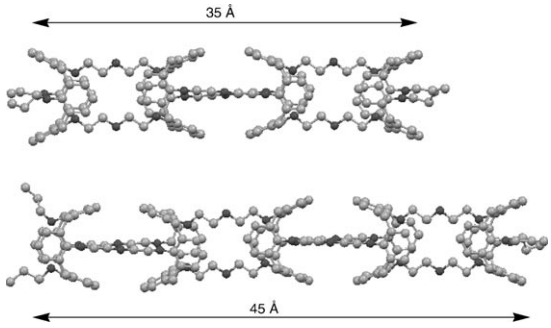

Figure 1. MacroModel 7.1 (Amber* Force Field) representation of nanotubular structures **3** and **4**, a side view. Hydrogen atoms removed for clarity. The X-ray structures of shorter tubes **1** and **2** have been reported.[7a]

Encapsulation studies: For monitoring the entrapment processes in SWNTs, a combination of different spectroscopic and microscopic techniques has been applied.[6] Especially important are TEM and FTIR spectroscopy, as they allow the internal location of molecules and their molecular vibrations, respectively, to be studied. Solution studies with SWNTs are still a challenge because of their poor solubility. Monitoring trapped guests by conventional spectroscopy in synthetic nanotubes has also been difficult. For example, the first calixarene-derived nanotubes, designed as channels for small metal ions, showed only weak complexation abilities, as the calixarene tunnel did not bind metal cations (Ag^+, K^+, Cs^+).[2] The situation is different when calixarenes and NO_x gases are employed. As mentioned earlier, simple calix[4]arenes reversibly interact with NO_2/N_2O_4 and entrap the reactive NO^+ cation within their π-electron-rich interiors.[10] Stable nitrosonium complexes, for example, **14**, were quantitatively isolated upon addition of a Lewis acid ($SnCl_4$).

Our findings with nanotubes **1**–**4** are as follows:

1) Addition of an excess of NO_2/N_2O_4 to nanotubes **1**–**4** in $(CHCl_2)_2$ in the presence of $SnCl_4$ or $BF_3{\cdot}Et_2O$ resulted in quantitative formation of nitrosonium complexes **1**·$(NO^+)_2$–**4**·$(NO^+)_5$ (Scheme 3). Similar complexes formed when nanotubes **1**–**4** were mixed with commercially available nitrosonium salt $NO^+SbF_6^-$ in $(CHCl_2)_2$. Complexes **1**·$(NO^+)_2$–**4**·$(NO^+)_5$ were identified by UV/Vis, FTIR, and ^1H NMR spectroscopy. They possess typi-

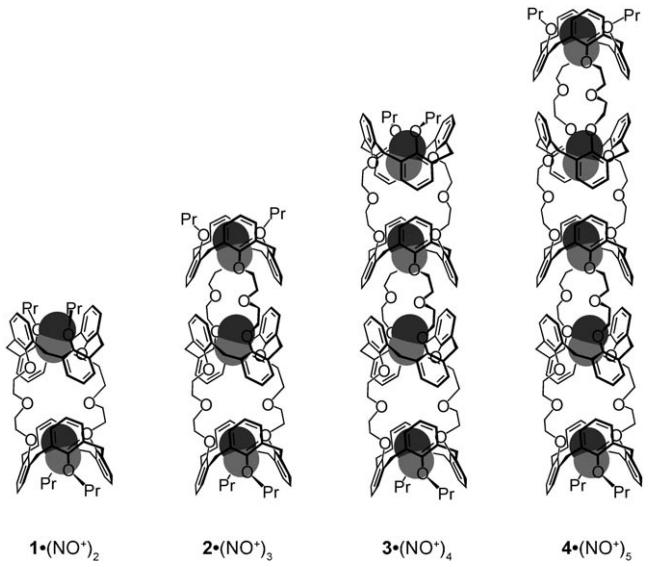

Scheme 3. Nitrosonium complexes of calixarene-based nanotubes. Counterions omitted for clarity. When NO_2/N_2O_4 is used as a source of NO^+, multiple NO_3^- counterions are formed, which are situated outside the tubes.

cal features of simpler calix[4]arene–NO^+ species, described earlier.[9,10]

2) Of particular importance is the characteristic deep purple color. The broad charge-transfer bands responsible for this are observed at $\lambda_{max} \approx 550$ nm in the absorption spectra of all these nanotubes. Charge transfer only occurs when NO^+ guests are tightly entrapped inside the calixarene cavities.[9,10] Accordingly, the filling process can be monitored visually. Upon stepwise addition of NO_2/N_2O_4 or $NO^+SbF_6^-$ in $(CDCl_2)_2$, the ^{1}H NMR signals of empty tubes **1**–**4** and complexes **1**·$(NO^+)_2$–**4**·$(NO^+)_5$ can be seen separately and in slow exchange. This is typical for host–guest complexes with high exchange barriers ($\Delta G^{\neq} > 15$ kcal mol^{-1}) and/or large association constants ($K_{assoc} > 10^6$ M^{-1}).[4a,b]
3) The presence of the guests and their location inside nanotubes **1**·$(NO^+)_2$–**4**·$(NO^+)_5$ can be deduced from conventional NMR analysis (Figure 2). Structural groups involved in complexation were identified by ^{1}H NMR, COSY, and NOESY experiments. Chemical shifts of the ArOCH_2 and CH_2OCH_2 protons, situated between $\delta =$ 2.5 and 3.75 ppm, and to a lesser extent the aromatic protons are very sensitive to encapsulation. In addition to charge transfer, strong cation–dipole interactions between the calixarene oxygen atoms and the entrapped NO^+ take place. All three groups of signals for the propyl ArOPr protons in **1**·$(NO^+)_2$–**4**·$(NO^+)_5$ were shifted significantly downfield ($\Delta\delta \approx 1$ ppm) relative to the signals obtained from empty tubes **1**–**4** (Figure 2). This implies that two NO^+ ions are located at the ends of the nanotubes and occupy the terminal calixarene compartments. Downfield shifts ($\Delta\delta > 1$ ppm) of the glycol ArOCH_2 and CH_2OCH_2 protons, situated in the middle of the tubular structures, were also observed. This indicated that the middle calixarene(s) in the longer tubes are filled with NO^+ as well.
4) According to molecular modeling, the NO^+-filled nanotubes **1**·$(NO^+)_2$–**4**·$(NO^+)_5$ adopt somewhat shrunken structures with all-*gauche* conformations about the glycol C–C bonds, whereas empty tubes **1**–**4** have all-*anti* C–C conformations, which was also evident from the X-ray structures of shorter tubes **1** and **2**.[7a] Experimental proof came from FTIR studies in $(CHCl_2)_2$ and CCl_4. In empty tubes **1**–**4** the band corresponding to the *anti* C–C conformation at $\tilde{\nu} = 1335$ cm^{-1} was observed. In complexes **1**·$(NO^+)_2$–**4**·$(NO^+)_5$ this band disappeared and a new band at $\tilde{\nu} = 1355$ cm^{-1} appeared, which is characteristic for the *gauche* C–C conformer (Figure 3). These absorptions are attributed to CH_2 wagging.[13] One reasonable explanation for such conformational change might be participation of the basic glycol CH_2OCH_2 oxygen atoms in NO^+ complexation. To appear in close proximity and thus contribute to dipole–cation interactions with entrapped NO^+, the glycol chains should adopt the more compact *gauche* C–C conformation (Figure 3, right). As a consequence, the filled nanotubes are shorter. This shrinkage brings the aromatic rings of neighboring calixarene units closer.[14] The *para* aromatic CH protons of tubes **1**·$(NO^+)_2$–**4**·$(NO^+)_5$ that face each other appear shielded and are seen somewhat upfield, at $\delta = 6.2$–6.4 ppm (Figure 2). These signals can be used as a characteristic signature for complex formation.
5) Complexation of NO^+ apparently does not influence the symmetry of nanotubes **1**–**4** (at 295 ± 5 K). The number of the propyl OCH_2, glycol CH_2OCH_2 and $ArOCH_2$, and aromatic ^{1}H NMR signals (Figure 2) for **1**·$(NO^+)_2$–**4**·$(NO^+)_5$ does not change, and this implies that the NO^+ guests, with van der Waals dimensions of about 2 Å, freely rotate along the N–O axis and also tumble within the cavity at room temperature.[15] Similar dynamics were

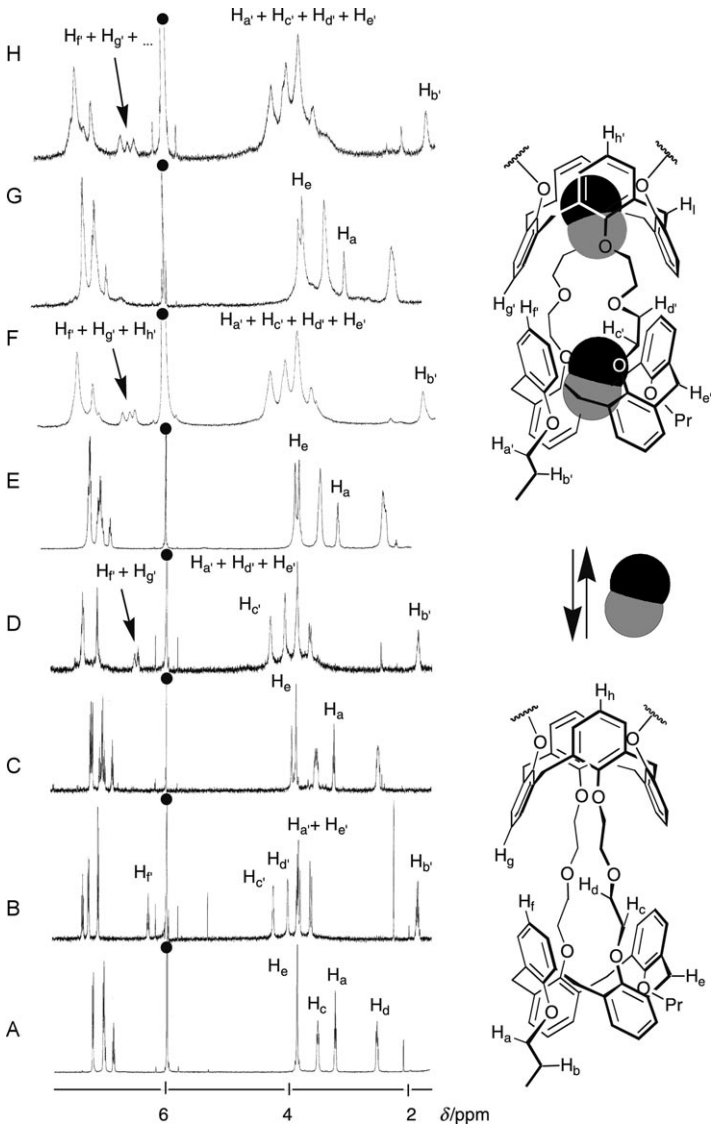

Figure 2. Selected portions of the ^{1}H NMR spectra (500 MHz, $(CDCl_2)_2$, 295 K) of A) nanotube **1**, B) filled nanotube **1**·$(NO^+)_2$, C) nanotube **2**, D) filled nanotube **2**·$(NO^+)_3$, E) nanotube **3**, F) filled nanotube **3**·$(NO^+)_4$, G) nanotube **4**, and H) filled nanotube **4**·$(NO^+)_5$. The residual solvent signals are marked with filled circles. Complexes **1**·$(NO^+)_2$–**4**·$(NO^+)_5$ were prepared from empty tubes **1**–**4** and NO_2/N_2O_4 in the presence of $SnCl_4$.

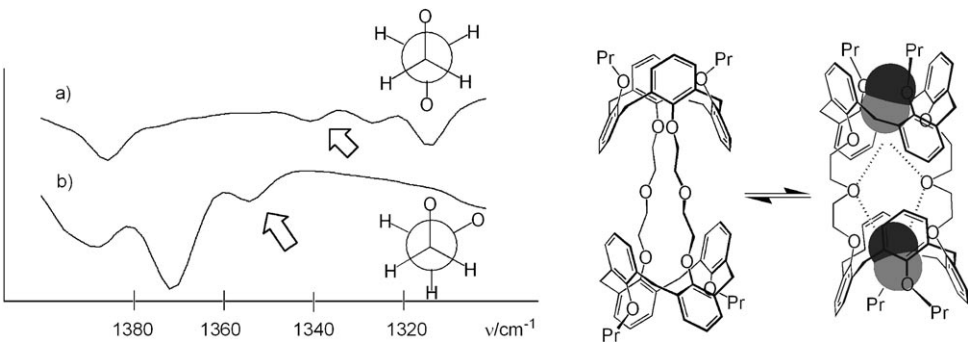

Figure 3. Portions of the IR spectra (in $(CHCl_2)_2$, 295 K) of A) empty tube **1** and B) filled tube **1**·$(NO^+)_2$. The bands corresponding to the *anti* and *gauche* C– conformations are marked. The band at $\tilde{\nu} = 1370\ cm^{-1}$ belongs to *tert*-butyl nitrite. Right: proposed conformational changes in the nanotubes upon complexation.

previously noticed for simpler calixarene–NO^+ complexes such as **14**.[9,10]

Stoichiometry: Thus far, we used NO_2/N_2O_4 gases to fill nanotubes **1**–**4** with multiple NO^+ guest species and followed the process by conventional spectroscopic techniques in solution. NO_2 and N_2O_4 are aggressive and difficult to handle in small, precise quantities. Moreover, they react with nanotubes upon standing and nitrosate/nitrate the aromatic rings. All this complicates the stoichiometric studies. Initially, by molecular modeling and analogy with simpler calixarene–NO^+ complexes (see **14**, for example),[9,10] it was suggested that one calixarene fragment in the nanotubes can accommodate only one NO^+. Accordingly, nanotubes **1**·$(NO^+)_2$–**4**·$(NO^+)_5$ should have two, three, four, and five NO^+ ions, respectively. Higher stoichiometries of NO^+ were ruled out: there is simply no room to accept a larger number of mutually repulsive cations.

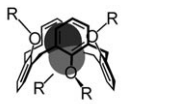

14a R = *n*-Hex
14b R = $CH_2CH_2OCH_3$

Recently, we found more reliable sources of NO^+ for determination of stoichiometry: alkyl nitrites (RON=O).[16] Alkyl nitrites are known as effective NO donors in medicine and they also act as nitrosating reagents.[17] We now report that NO^+ can be quantitatively transferred from alkyl nitrites into calixarene nanotubes **1**–**4**. Alkyl nitrites are much easier to handle than NO_2/N_2O_4 gases. They are stable, nonvolatile liquids that are easy to transfer by conventional laboratory pipettes.

Preliminary experiments with simple calix[4]arenes and shorter tubes were recently published.[16] In short, addition of *tert*-butyl nitrite to solutions of tetrakis(*O*-*n*-hexyloxy)calix[4]arene in $CDCl_3$ or nanotubes **1** and **2** in $(CDCl_2)_2$ in the presence of an excess of $SnCl_4$ or trifluoroacetic acid (TFA) led to rapid, quantitative formation of the corresponding calixarene–NO^+ complexes. These were identified by means of NMR, FTIR, and UV/Vis spectra, which showed features similar to those of the previously described tubes **1**·$(NO^+)_2$ and **2**·$(NO^+)_3$, filled with the help of NO_2/N_2O_4.[7] From the integration, it was possible to quantitatively estimate the concentration of complexes **1**·$(NO^+)_2$ and **2**·$(NO^+)_3$. Two equivalents of *tert*-butyl nitrite were needed to fill dimeric tube **1**, and adding three equivalents of the nitrite completely filled trimeric nanotube **2**. Analogously, 1:4 stoichiometry was established for longer tube **3** having four calix-

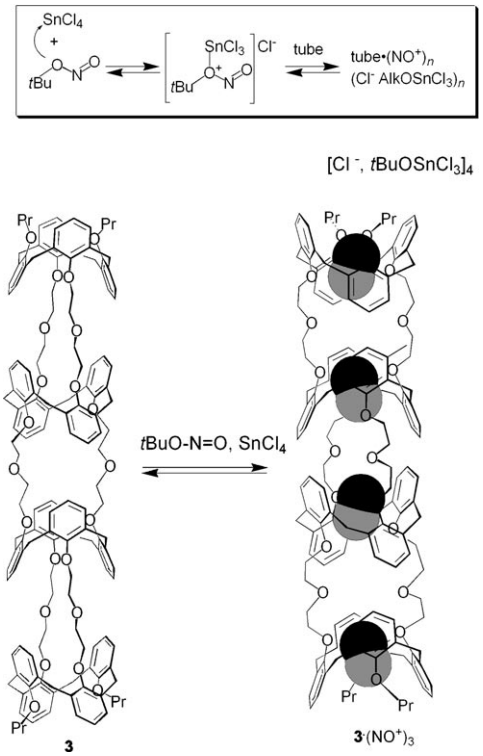

Scheme 4. Filling synthetic nanotubes through supramolecular nitrosonium transfer with *tert*-butyl nitrite and $SnCl_4$.

arene units (Scheme 4). Further addition of the nitrite did not change the NMR spectra. This confirms the stoichiometry of the nanotube complexes, which thus have one NO^+ per calixarene unit. A similar trend is expected for longer tube **4**, although the titrations in this case are less accurate due to broadening of signals and rather low solubility of the complex.

Transfer of NO^+ does not occur in the absence of $SnCl_4$. Most probably, the Lewis acid interacts with the nitrite CON oxygen atom and facilitates breaking the O–N bond (Scheme 4, top). It may also stabilize the complexes by coordinating to the counterion, similar to known arene nitrosonium nitrate complexes.[18]

On the binding strength: We noticed that complexes $\mathbf{1}\cdot(NO^+)_2$–$\mathbf{3}\cdot(NO^+)_4$ form in significant quantities even when less than stoichiometric amounts of *tert*-butyl nitrite are added. For example, addition of one equivalent of *tert*-butyl nitrite to dimeric tube **1** produces $50\pm5\%$ of fully occupied complex $\mathbf{1}\cdot(NO^+)_2$, and addition of two equivalents of *tert*-butyl nitrite to trimeric tube **2** produces $55\pm5\%$ of fully occupied complex $\mathbf{2}\cdot(NO^+)_3$, which is much higher than in a simple statistical distribution. Furthermore, partially filled complexes were not detected. This suggests cooperativity. With the complexation of the first NO^+ guest(s), the nanotube structure becomes more rigid and preorganized due to conformational changes of the glycol linkers from *anti* to *gauche* (see Figure 3). In such conformational transition, the glycol oxygen atoms become more preorganized for further interactions with the entrapped NO^+ species.[19,20]

Vibrational spectra allowed us to obtain independent, unique information on the bonding of multiple NO^+ species inside tubes $\mathbf{1}\cdot(NO^+)_2$–$\mathbf{4}\cdot(NO^+)_5$ in solution. From the literature, the nitrosonium salts NO^+Y^- ($Y^-=BF_4^-$, PF_6^-, AsF_6^-) show a single stretching band at $\tilde{\nu}(NO^+)=2270\,cm^{-1}$ in CH_3NO_2 solution,[21] and the stretching frequency of neutral diatomic NO gas is $\tilde{\nu}(NO)=1876\,cm^{-1}$.[21] In calixarene–$NO^+$ complexes **14**, the NO^+ band significantly shifted ($\Delta\nu=312\,cm^{-1}$) to lower energies compared to free NO^+ ion and appeared at $\tilde{\nu}(NO^+)=1958\,cm^{-1}$ in $(CHCl_2)_2$ (Figure 4). This is due to strong electron donor–acceptor interactions between encapsulated NO^+ and the π-electron-rich aromatic walls of the calixarene.[9] Dimeric complex $\mathbf{1}\cdot(NO^+)_2$ also exhibited similar shifts for the NO^+ guests at $\tilde{\nu}(NO^+)=1958\,cm^{-1}$. At the same time, longer tubes $\mathbf{2}\cdot(NO^+)_3$–$\mathbf{4}\cdot(NO^+)_5$ clearly showed two absorption bands at $\tilde{\nu}(NO^+)=1958\,cm^{-1}$ and $1940\,cm^{-1}$ in $(CHCl_2)_2$. For trimeric tube $\mathbf{2}\cdot(NO^+)_3$, these two bands have a comparable intensity, while in longer tubes $\mathbf{3}\cdot(NO^+)_4$ and $\mathbf{4}\cdot(NO^+)_5$ the band at $\tilde{\nu}(NO^+)=1940\,cm^{-1}$ dominates. This band was assigned to the NO^+ guest(s) situated in the middle of the tubes. Apparently, they are somewhat more strongly bound to the nanotube walls. One possible explanation is participation of the glycol CH_2OCH_2 oxygen atoms (Figure 3). As discussed earlier for the *anti–gauche* conformational transition upon complexation, these oxygen atoms are in close proximity and thus contribute to dipole–cation interactions with the entrapped NO^+. Interestingly, in calixarene–NO^+ complex **14b**, which models the middle part of the filled tubes, the NO^+ band only appeared at $\tilde{\nu}(NO^+)=1958\,cm^{-1}$ in $(CHCl_2)_2$. Apparently, the tubular structures in $\mathbf{2}\cdot(NO^+)_3$–$\mathbf{4}\cdot(NO^+)_5$ offer more rigidity and enhance complexation. Possible cooperativity through allosteric effects is currently under further investigation. It may be the result of multiple guests aligning in one dimension, which brings an order that cannot be achieved for shorter complexes.

Guest exchange and dynamics: Filled nanotubes $\mathbf{1}\cdot(NO^+)_2$–$\mathbf{4}\cdot(NO^+)_5$ are stable in dry solution at room temperature for hours, but readily dissociate upon addition of H_2O or MeOH, quantitatively producing free **1**–**4**. The process, however, is not reversible: the released NO^+ are now converted to nitrous acid and complexes $\mathbf{1}\cdot(NO^+)_2$–$\mathbf{4}\cdot(NO^+)_5$ cannot be regenerated.

We further found that [18]crown-6 can remove the encapsulated NO^+ species (Scheme 5). It is known that crown ethers form stable complexes with NO^+.[22] When about four equivalents of [18]crown-6 were added to solutions of $\mathbf{1}\cdot(NO^+)_2$ and $\mathbf{2}\cdot(NO^+)_3$ in $(CDCl_2)_2$, empty nanotubes **1** and **2**, respectively, regenerated within minutes, and the deep purple color disappeared. The process can be followed by ^1H NMR spectroscopy (Figure 5). Interestingly, further addition of $SnCl_4$ to the same solutions fully restores complexes $\mathbf{1}\cdot(NO^+)_2$ and $\mathbf{2}\cdot(NO^+)_3$. That $SnCl_4$ forms complexes with crown ethers is well documented.[23] In our hands, the addition of four equivalents of $SnCl_4$ to a solution containing only [18]crown-6 ($\delta=3.6$ ppm) in $(CDCl_2)_2$ resulted in a new [18]crown-6 singlet at $\delta=3.7$ ppm. This indicates strong interaction between $SnCl_4$ and [18]crown-6 in solution.

Apparently in our case, an excess of $SnCl_4$ displaces NO^+ from the crown ether moiety,

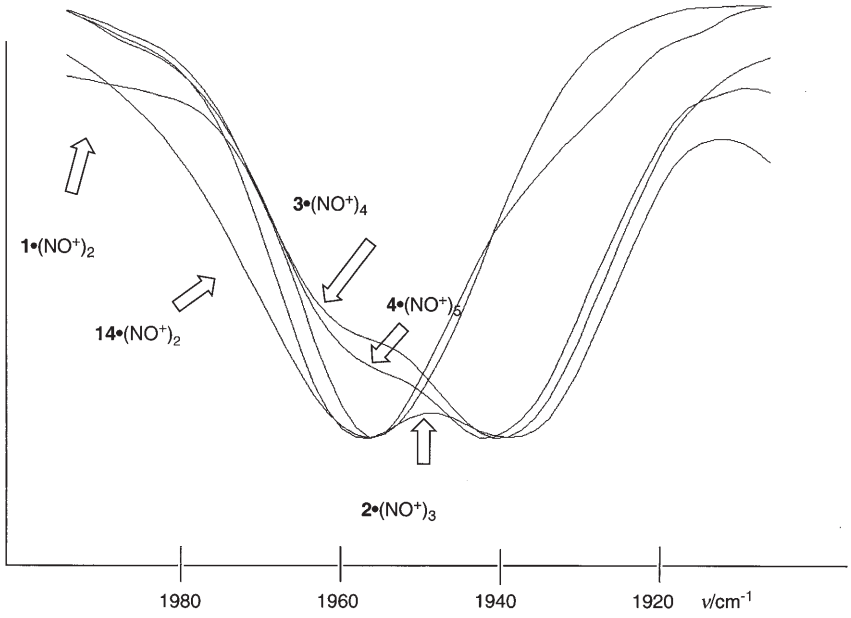

Figure 4. Selected portions of the IR spectra (in $(CHCl_2)_2$, 295 K) of calixarene complex **14a** and completely filled nanotubes $\mathbf{1}\cdot(NO^+)_2$–$\mathbf{4}\cdot(NO^+)_5$. Calixarene complex **14b** looks similar to **14a**. For the filling experiments, *tert*-butyl nitrite and $SnCl_4$ were used.

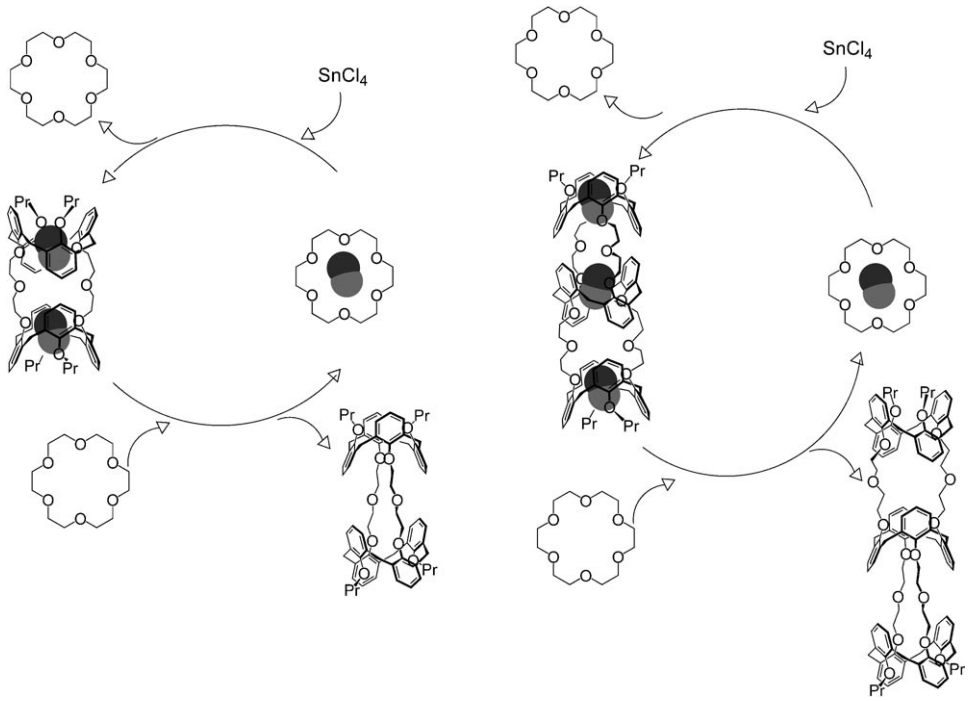

Scheme 5. Nitrosonium exchange in calixarene nanotubes involving [18]crown-6 and $SnCl_4$.

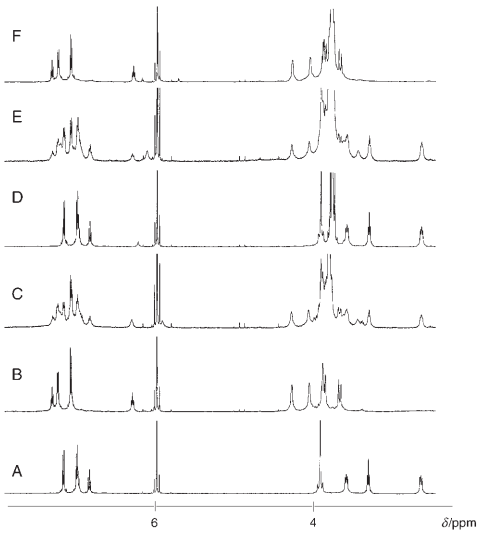

Figure 5. Nitrosonium exchange. Selected portions of the ^{1}H NMR spectra (500 MHz, $(CDCl_2)_2$, 295 K) of A) nanotube **1** and B) filled nanotube **1**·$(NO^+)_2$. C) Same as B) with 1 equiv of [18]crown-6. D) Same as B) with 2 equiv of [18]crown-6. E) same as D) with 2 equiv of $SnCl_4$. F) Same as D) with 4 equiv of $SnCl_4$.

and the latter goes back to the calixarene units of the nanotubes. This observation is important, since in this case foreign species can be replaced and returned without decomposition or changing the polarity of the solution.

The guest-exchange mechanism is currently under investigation. Modeling suggests that NO^+ can enter and leave the nanotube through either its ends or the middle gates between the calixarene modules.[24] Approach and exit through the ends appears to be less hindered. The middle gates between the calixarene units become narrower due to the conformational change of the glycol moieties from *anti* to *gauche* upon complexation (see Figure 3). The encapsulated NO^+ should also avoid electrostatic repulsions with each other. Most probably, tube filling and release occurs through the guest tunneling along the interior, which may be common to all nanotubes.

Conclusions and Outlook

Long synthetic nanotubes are now readily available that can be used for filling purposes. The nanotubes reported here are based on calix[4]arenes and take advantage of their extremely diverse, high-yield chemistry. These nanotubes reversibly interact with NO_x gases and thus can be filled with multiple nitrosonium guests.[25] The major feature of these tubes is the ability to align multiple guest species in one dimension. This brings an order that cannot be achieved for simpler and shorter complexes. It may also influence guest exchange into and out of the nanotubes, as well as the binding strength. Among possible applications are the design of synthetic nanowires and optical sensors for NO_x. Chemical fixation of NO_x is also of great interest.[26] The tubes can be used for molecular storage of active nitrosonium ions and act as size- and shape-selective nitrosating reagents.[27] Generation of NO gas inside these nanotubes and its release is also possible.[28] We are currently working in these directions.

Finally, in contrast to other molecular containers,[4] supramolecular chemistry of synthetic nanotubes is still not explored. Their unique geometrical features and nanosize, which allow for the simultaneous entrapment of multiple guests in a one-dimensional fashion, places them in a unique position to uncover novel phenomena in molecular encapsulation.[29,30]

Experimental Section

General: Melting points were determined on a Mel-Temp apparatus (Laboratory Devices, Inc.) and are uncorrected. ^{1}H, ^{13}C NMR, COSY, and NOESY spectra were recorded at 295 ± 1 °C on JEOL 300 and 500 MHz spectrometers. Chemical shifts were measured relative to residual undeuterated solvent resonances. FTIR spectra were recorded on a Bruker Vector 22 FTIR spectrometer. UV/Vis spectra were measured on

a Varian Cary-50 spectrophotometer. Mass spectra were recorded at the Scripps Center for Mass Spectrometry (La Jolla, CA). High-resolution MALDI FT mass spectra were obtained on an IonSpec Ultima FTMS. MALDI TOF mass spectra were obtained on an Applied Biosytems Voyager STR (2). Elemental analysis was performed on a Perkin–Elmer 2400 CHN analyzer. All experiments with moisture- and/or air-sensitive compounds were run under a dried nitrogen atmosphere. For column chromatography, silica gel 60 Å (Sorbent Technologies, 200–425 mesh) was used. Parent tetrahydroxycalix[4]arene[31] and calixarene **14b**[32] were prepared according to the published procedures. NO_2/N_2O_4 was generated from copper and concentrated HNO_3. Molecular modeling was performed using commercial MacroModel 7.1 with Amber* Force Field.[33]

Caution: NO_2 has an irritating odor and is very toxic!

25,27-Bis[2-benzyloxy)ethyloxy]-26,28-dihydroxycalix[4]arene (9): A suspension of parent calix[4]arene (1.0 g, 2.4 mmol), 2-(benzyloxy)ethanol *p*-toluenesulfonate (1.51 g, 4.94 mmol), and K_2CO_3 (0.67 g, 4.8 mmol) in MeCN (20 mL) was refluxed for 24 h. After cooling to RT, the solvent was removed under reduced pressure, and the residue was treated with 10% aqueous HCl (20 mL) and CH_2Cl_2 (40 mL). The organic layer was separated and washed with 10% aqueous $NaHCO_3$ (2×15 mL) and brine. The organic solution was dried over $MgSO_4$, filtered, and evaporated in vacuo. The resulting pale yellow oil solidified upon addition of MeOH (3×15 mL) to give **9** as a white powder. Yield: 1.158 g (71%); m.p. 138–140°C; ^{1}H NMR (500 MHz, $CDCl_3$): δ=7.87 (s, 2H; ArOH), 7.33 (m, 10H; ArH), 7.06, 6.89 (2×d, J=7.5 Hz, 8H; ArH_m), 6.72, 6.65 (2×t, J=7.5 Hz, 4H; ArH_p), 4.65 (s, 4H; $ArCH_2O$), 4.45, 3.37 (2×d, J=12.8 Hz, 8H; $ArCH_2Ar$), 4.18 (t, J=5.1 Hz, 4H; OCH_2CH_2O), 3.92 ppm (t, J=5.1 Hz, 4H; OCH_2CH_2O); ^{13}C NMR ($CDCl_3$): δ=153.4, 152.0, 138.2, 133.4, 129.0, 128.6, 128.5, 128.2, 128.0, 127.7, 125.4, 118.9, 75.7, 73.7, 69.2, 31.4 ppm; FTIR (KBr): ν=3333, 3062, 3028, 2928, 2861, 1467, 1453, 1355, 1250, 1200, 1123, 1090, 1045 cm^{-1}; elemental analysis calcd (%) for $C_{46}H_{46}O_6$: C 79.51, H 6.67; found: C 79.23, H 6.41.

25,27-Bis[2-benzyloxy)ethyloxy]-26,28-bis[2-(*tert*-butyldimethylsiloxy)ethyloxy]calix[4]arene (1,3-alternate conformer 10): A suspension of calix[4]arene **9** (1.15 g, 1.65 mmol) and Cs_2CO_3 (2.7 g, 8.3 mmol) in DMF (30 mL) was heated at 90°C for 1 h, then a solution of 2-(*tert*-butyldimethylsiloxy)ethanol *p*-toluenesulfonate (2.74 g, 8.29 mmol) in DMF (10 mL) was added. The reaction mixture was stirred at 90°C for 24 h. DMF was completely removed in vacuo, and the reaction mixture was treated with 10% aqueous acetic acid (50 mL) and CH_2Cl_2 (50 mL). The organic layer was separated, washed with 10% aqueous $NaHCO_3$ (15 mL) and brine, (2×15 mL), and dried over $MgSO_4$. Evaporation of CH_2Cl_2 gave a light yellow solid, which was refluxed with KI (1 g) and Et_3N (1 mL) in MeCN (30 mL) for 1 h. The solvent was evaporated in vacuo, and the residue solidified upon addition of MeOH (3×15 mL). The resulting brownish yellow solid was then refluxed with MeOH (25 mL), filtered hot, and washed with MeOH (3×15 mL) to give **10** as a white powder. Yield: 1.12 g (67%); m.p. 116–120°C; ^{1}H NMR (500 MHz, $CDCl_3$): δ=7.36 (m, 10H; ArH), 7.07, 7.04 (2×d, J=7.3 Hz, 8H; ArH_m), 6.62, 6.56 (2×t, J=7.3 Hz, 4H; ArH_p), 4.66 (s, 4H; $ArCH_2O$), 3.87 (m, 8H; OCH_2CH_2O), 3.77, 3.71 (2×m, 8H; OCH_2CH_2O), 3.55 (m, 8H; $ArCH_2Ar$), 0.96 (s, 18H; *t*Bu), 0.15 ppm (s, 12H; CH_3); ^{13}C NMR ($CDCl_3$): δ=155.8, 155.6, 138.4, 133.6, 130.0, 129.8, 128.5, 127.8, 121.9, 74.0, 73.4, 71.6, 69.7, 62.7, 34.9, 26.2, 18.5, −5.1 ppm; FTIR ($CHCl_3$): $\tilde{\nu}$=3068, 3032, 2931, 2714, 1452, 1361, 1250, 1198, 1098, 1029 cm^{-1}; elemental analysis calcd (%) for $C_{62}H_{80}O_8Si_2$: C 73.77, H 7.99; found: C 73.52, H 7.93.

25,27-Bis[2-benzyloxy)ethyloxy]-26,28-bis[2-(hydroxy)ethyloxy]calix[4]arene (1,3-alternate conformer 11): Acetyl chloride (0.51 g, 0.46 mL, 6.5 mmol) was added dropwise to ice-cold CH_2Cl_2/MeOH (10 mL, 9/1 v/v), and after 30 min a solution of calix[4]arene **10** (1.1 g, 1.1 mmol) in CH_2Cl_2 (5 mL) was added. After the starting material was consumed (TLC, hexane/AcOEt, 7/3, ca. 1 h), the reaction mixture was washed with 10% aqueous $NaHCO_3$ (5 mL) and brine (5 mL) and dried over $MgSO_4$. The residue was purified by column chromatography (CH_2Cl_2/MeOH, 96/4, R_f=0.2) to give **11** as a colorless solid. Yield: 0.74 g (87%); m.p. 174–176°C; ^{1}H NMR (500 MHz, $CDCl_3$): δ=7.33 (m, 10H; ArH), 7.07, 7.00 (2×d, J=7.3 Hz, 8H; ArH_m), 6.91, 6.68 (2×t, J=7.3 Hz, 4H; ArH_p), 4.38 (s, 4H; $ArCH_2O$), 3.85 (AB q, J=16.9 Hz, 8H; $ArCH_2Ar$), 3.6 (m, 8H; OCH_2CH_2O), 3.30 (t, J=6.0 Hz, 4H; OCH_2CH_2O), 2.91 (t, J=6.0 Hz, 4H; OCH_2CH_2O), 1.68 ppm (br s, 2H; OH); ^{13}C NMR ($CDCl_3$): δ=156.3, 156.1, 138.4, 133.8, 133.7, 129.5, 129.4, 128.5, 127.9, 127.8, 127.6, 123.2, 123.0, 73.2, 71.4, 68.1, 61.3, 38.0 ppm; FTIR ($CHCl_3$): $\tilde{\nu}$=3529, 3421, 3066, 3033, 2927, 2872, 1468, 1365, 1324, 1247, 1215, 1092, 1037 cm^{-1}; elemental analysis calcd (%) for $C_{50}H_{52}O_8$: C 76.90, H 6.71; found: C 76.82, H 6.66.

Bis(1-propyloxy)bis[2-benzyloxy(ethyloxy)]calix[4]tube (13): Calix[4]arene **11** (0.12 g, 0.153 mmol) was dissolved in dry THF (40 mL), and NaH (60% suspension in mineral oil, 0.61 g, 1.5 mmol) was added. The mixture was stirred at 45°C for 1 h, after which a solution of calix[4]arene **12**[12] (0.14 g, 0.15 mmol) in THF (20 mL) was added slowly over 4 h. The reaction mixture was refluxed for 24 h. After cooling, the solvent was evaporated under reduced pressure and CH_2Cl_2 (30 mL) and 10% aqueous HCl (10 mL) were added. The organic layer was washed with 10% aqueous $NaHCO_3$ (10 mL) and a saturated solution of NaCl (2×10 mL), dried over $MgSO_4$, and evaporated in vacuo. The residue was purified by column chromatography with CH_2Cl_2/MeOH (99/1, R_f=0.3) as eluent to afford **13** as a colorless solid. Yield: 0.064 g (32%); m.p. >270°C (decomp); ^{1}H NMR (500 MHz, $CDCl_3$): δ=7.3 (m, 10H; ArH), 7.17, 7.16 (2×d, J=7.5 Hz, 8H; ArH), 7.02 (m, 12H; ArH), 6.85, 6.72 (2×t, J=7.5 Hz, 4H; ArH), 4.31 (s, 4H; $ArCH_2O$), 3.90 (AB q, J=16.5 Hz, 8H; $ArCH_2Ar$), 3.88 (AB q, J=16.5 Hz, 8H; $ArCH_2Ar$), 3.56 (m, 8H; OCH_2CH_2O), 3.48, 3.31, 2.92 (3×t, J=6.5 Hz, 12H; OCH_2CH_2O, OCH_2), 2.57 (m, 8H; OCH_2CH_2O), 1.06 (m, 4H; CH_2), 0.56 ppm (t, J=7.3 Hz, 6H; CH_3); ^{13}C NMR ($CDCl_3$): δ=157.3, 156.6, 155.9, 155.8, 134.2, 134.1, 134.0, 129.1, 129.0, 128.9, 128.8, 128.5, 127.7, 127.6, 122.9, 122.8, 122.5, 122.0, 73.1, 71.5, 69.1, 68.5, 68.2, 66.1, 66.0, 38.3, 38.1, 22.7, 10.2 ppm; FTIR ($CHCl_3$): ν=3065, 3033, 2925, 2875, 1462, 1247, 1215, 1124, 1094, 1034, 1009 cm^{-1}; MALDI-FTMS: *m/z*: 1363.6439 $[M+Na]^+$; calcd for $C_{88}H_{92}O_{12}Na$: 1363.6486.

Bis(1-propyloxy)bis[2-hydroxy(ethyloxy)]calix[4]tube (7): A mixture of 10 wt% Pd/C (0.03 g), the above-described benzylated calix[4]tube **13** (0.06 g, 0.044 mmol), and AcOH (0.1 mL) in THF (5 mL) was stirred under H_2 (1 atm) at RT until all starting material disappeared (TLC, CH_2Cl_2/MeOH, 99/1). The suspension was filtered through Celite and the clear solution was concentrated in vacuo. The residue was triturated with MeOH (3×2 mL) to afford **7** as a white powder. Yield: 0.042 g (82%); m.p. >300°C (decomp); ^{1}H NMR (500 MHz, $CDCl_3$): δ=7.21, 7.15 (2×d, J=7.6 Hz, 8H; ArH), 7.05 (m, 12H; ArH), 6.95, 6.86 (2×t, J=7.6 Hz, 4H; ArH), 3.95 (AB q, J=17.2 Hz, 8H; $ArCH_2Ar$), 3.88 (AB q, J=16.5 Hz, 8H; $ArCH_2Ar$), 3.63 (t, J=7.0 Hz, 4H; OCH_2CH_2O), 3.56 (m, 8H; OCH_2CH_2O), 3.31 (t, J=7.0 Hz, 4H; OCH_2), 3.21(m, 4H; OCH_2CH_2O), 2.56 (m, 8H; OCH_2CH_2O), 2.27 (br s, 2H; OH), 1.06 (m, 4H; CH_2), 0.56 ppm (t, J=7.6 Hz, 6H; CH_3); ^{13}C NMR ($CDCl_3$): δ=157.3, 156.4, 156.0, 155.8, 134.2, 134.0, 133.9, 133.5, 129.2, 129.1, 128.9, 128.8, 123.6, 123.0, 122.8, 121.9 ppm; FTIR (KBr): ν=3529, 3453, 3060, 3030, 3011, 2924, 2875, 1459, 1216, 1132, 1094, 1035, 1011 cm^{-1}; MALDI-FTMS: *m/z* 1183.5426 $[M+Na]^+$; calcd for $C_{74}H_{80}O_{12}Na$: 1183.5547.

Bis(1-propoxy)bis[2-(*p*-toluenesulfonyloxy)ethoxy]calix[4]tube (8): calix[4]tube **7** (0.11 g, 0.095 mmol), DMAP (0.046 g, 0.38 mmol), and *p*-toluenesulfonyl chloride (0.070 g, 0.38 mmol) were dissolved in CH_2Cl_2 (15 mL) and cooled to −5°C. Triethylamine (0.20 mL) was added, and the solution was stirred overnight at RT. The solution was evaporated to dryness, the residue redissolved in CH_2Cl_2, and the resulting solution washed with 5% HCl, water, and brine. The organic layer was dried with Na_2SO_4 and evaporated to dryness. Treatment with MeOH produced **8** as a colorless solid. Yield: 0.12 g (86%); m.p. 242–243°C; ^{1}H NMR (500 MHz, $CDCl_3$): δ=7.79 (d, J=8.4 Hz, 4H; ArH_{tosyl}), 7.40 (d, J=8.4 Hz, 4H; ArH_{tosyl}), 7.17, 7.15 (2×d, J=1.7 Hz, 8H; ArH), 7.06–6.97 (t+d+t, 8H; ArH), 6.94 (d, J=7.3 Hz, 4H; ArH), 6.86 (t, J=7.3 Hz, 2H; ArH_p), 6.69 (t, J=7.3 Hz, 2H; ArH_p), 3.89–3.80 (m, 16H; $ArCH_2Ar$), 3.57 (m, 12H; OCH_2CH_2O), 3.39 (m, 4H; OCH_2CH_2O), 3.32 (t, J=7.3 Hz, 4H; OCH_2), 2.57 (m, 8H; OCH_2CH_2O), 2.48 (s, 6H; $ArCH_3$), 1.10 (m, 4H; CH_2), 0.58 ppm (t, J=7.3 Hz, 6H; CH_3); ^{13}C ($CDCl_3$): δ=157.3, 155.9, 155.8, 155.6, 145.0, 134.2, 134.0, 133.9, 133.8, 133.2, 130.0, 129.1, 129.0, 128.8, 128.0, 123.3, 122.9, 122.8, 121.9, 71.5,

69.1, 68.9, 67.8, 66.8, 66.2, 66.0, 38.3, 38.0, 22.7, 21.7, 10.2 ppm; FTIR (KBr): $\tilde{\nu}$ = 3061, 3031, 3014, 2959, 2918, 2874, 1459, 1214, 1177, 1095, 1033, 1011 cm^{-1}; elemental analysis calcd (%) for $C_{88}H_{96}O_{16}S_2$: C 71.71, H 6.57; found: C 71.78, H 6.46.

Trimeric tube 2: A solution of calix[4]arenes **5**[11] (100 mg, 0.08 mmol) and **6**[7b] (98 mg, 0.16 mmol) in THF (25 mL) was added dropwise to a suspension of NaH (60% in mineral oil, 26 mg, 1.3 mmol) in THF (150 mL) at 70°C over 8 h. The mixture was further refluxed for 4 d, evaporated to dryness, and the residue suspended in CH_2Cl_2 (50 mL) and neutralized at 0°C with 5% aqueous HCl (50 mL). The organic layer was washed with water (3×5 mL), dried over Na_2SO_4, and then evaporated to dryness. The residue was treated with MeCN to produce nanotube **2** as a white solid. Yield: 0.10 g (70%); m.p. >300°C (decomp); ^{1}H NMR (500 MHz, $CDCl_3$): δ = 7.20, 7.18 (2×d, J = 7.3 Hz, 16H; ArH_m), 7.08 (t, J = 7.3 Hz, 4H; ArH_p), 7.02 (d, J = 7.3 Hz, 8H; ArH_m), 6.98, 6.85 (2×t, J = 7.3 Hz, 8H; ArH_p), 3.94 (s, 8H; $ArCH_2Ar$), 3.88 (AB q, J = 16.5 Hz, 16H; $ArCH_2Ar$), 3.57 (m, 16H; $ArOCH_2CH_2O$), 3.30 (t, J = 7.3 Hz, 8H; OCH_2), 2.55 (m, 16H; $ArOCH_2CH_2O$), 1.06 (m, 8H; CH_2), 0.56 ppm (t, J = 7.3 Hz, 12H; CH_3); ^{13}C NMR ($C_2D_2Cl_4$): δ = 157.2, 156.2, 155.9, 134.2, 134.1, 134.0, 129.3, 129.1, 128.8, 122.9, 122.7, 122.0, 71.8, 70.9, 69.2, 66.7, 66.5, 38.3, 38.1, 22.8, 10.4 ppm; FTIR (CCl_4): $\tilde{\nu}$ = 3064, 3033, 3016, 2959, 2921, 2873, 1459, 1216, 1125, 1093, 1035, 1010 cm^{-1}; MALDI-FTMS: m/z: 1743.8443 $[M+Na]^+$; calcd for $C_{112}H_{120}O_{16}Na$: 1743.8473. This modified procedure reproducibly gave much better yields than the previously published protocol.[7a]

Tetrameric nanotube 3: A solution of calix[4]tubes **8** (57 mg, 0.039 mmol) and **7** (45 mg, 0.039 mmol) in THF (25 mL) was added dropwise over 1 h to a mixture of NaH (60% suspension in mineral oil, 12 mg, 0.31 mmol) and K_2CO_3 (22 mg, 0.16 mmol) in THF (100 mL) at reflux temperature. The mixture was further refluxed for 24 h, evaporated to dryness, suspended in CH_2Cl_2 (50 mL), and neutralized at 0°C with 5% HCl (25 mL). The organic layer was washed with water (2×5 mL), dried over Na_2SO_4, and then evaporated to dryness. The residue was treated with MeCN to produce **3** as a colorless solid. Yield: 56 mg (64%); m.p. >300°C (decomp); ^{1}H NMR (500 MHz, $(C_2D_2Cl_4)$: δ = 7.22, 7.19 (2×d, J = 7.3 Hz, 24H; ArH_m), 7.07–6.97 (m, 20H; ArH), 6.87 (t, J = 7.3 Hz, 4H; ArH_p), 3.94 (s, 16H; $ArCH_2Ar$), 3.88 (AB q, J = 17.6 Hz, 16H; $ArCH_2Ar$), 3.58 (m, 24H; $ArOCH_2CH_2O$), 3.28 (t, J = 7.3 Hz, 8H; OCH_2), 2.58 (m, 24H; $ArOCH_2CH_2O$), 1.09 (m, 8H; CH_2), 0.58 ppm (t, J = 7.3 Hz, 12H; CH_3); FTIR (CCl_4): ν = 3061, 3032, 3010, 2958, 2925, 2873, 1459, 1216, 1128, 1094, 1033, 1012 cm^{-1}; MS (MALDI-TOF): m/z: 2308 $[M+Na]^+$; calcd for $C_{148}H_{156}O_{22}Na$: 2308.

Pentameric nanotube 4: A solution of calix[4]arene **5**[11] (50 mg, 0.041 mmol) and calix[4]tube **7** (95 mg, 0.082 mmol) in THF (25 mL) was added dropwise over 1 h to a mixture of NaH (60% suspension in mineral oil, 13 mg, 0.33 mmol) and K_2CO_3 (22 mg, 0.16 mmol) in THF (100 mL) at reflux temperature. The mixture was further refluxed for 24 h, evaporated to dryness, suspended in CH_2Cl_2 (50 mL), and neutralized at 0°C with 5% HCl (25 mL). The organic layer was washed with water (2×5 mL), dried over Na_2SO_4, and then evaporated to dryness. The residue was treated with MeCN to produce pentacalix[4]tube **4** as a colorless solid. Yield: 96 mg (82%); m.p. >300°C (decomp); ^{1}H NMR (500 MHz, $CDCl_3$): δ = 7.20, 7.17 (2×d, J = 7.0 Hz, 32H; ArH), 7.09–6.98 (m, 24H; ArH), 6.87 (t, J = 7.3 Hz, 4H; ArH_p), 3.94 (s, 24H; $ArCH_2Ar$), 3.93 (AB q, J = 16.9 Hz, 16H; $ArCH_2Ar$), 3.62 (m, 32H; $ArOCH_2CH_2O$), 3.33 (t, J = 7.3 Hz, 8H; OCH_2), 2.58 (m, 32H; $ArCH_2CH_2O$), 1.11 (m, J = 7.3 Hz, 8H; CH_2), 0.58 ppm (t, J = 7.3 Hz, 12H; CH_3); FTIR (CCl_4): ν = 3063, 3033, 3016, 2958, 2926, 2874, 1459, 1217, 1128, 1094, 1033, 1010 cm^{-1}; MALDI-TOF MS: m/z: 2872 $[M+Na]^+$; calcd for $C_{184}H_{192}O_{28}Na$: 2872.

FTIR spectroscopy: In a general procedure, each compound was dissolved in $(CHCl_2)_2$ at 4×10^{-3} M, followed by the addition of two equivalents of $SnCl_4$ and two equivalents of *t*BuONO per calixarene unit. The spectra were recorded in solution by using an NaCl amalgamated sealed cell (1.0 mm) by coaddition of 20 scans, back and forward, at a resolution of 4 cm^{-1}. For each measurement, the solvent was used for background.

Titration experiments, typical procedure: An aliquot from the stock solution of *tert*-butyl nitrite (1.66 M) in $(CDCl_2)_2$ was added to an NMR tube containing a solution of calix[4]tube **3** (ca. 4 mM) and $SnCl_4$ or TFA (8 equiv) in $(CDCl_2)_2$, and after homogenization the spectrum was recorded. Additional aliquots of the nitrite were added and the spectrum was recorded after each addition. The *tert*-butyl nitrite concentration ranged between 2 and 25 mM. The concentration of complex **3**·$(NO^+)_4$ was determined by integration of the aromatic CH protons and/or the OCH_2 methylene protons versus the corresponding signals of free tube **3**. The experiments were performed at least in duplicate.

Acknowledgements

This research was supported by the National Science Foundation (CHE-0350958), the Texas Advanced Technology Program (003656-0146-2003), and the Alfred P. Sloan Foundation. We are also grateful to the NSF for funding the purchase of the 300 MHz NMR spectrometer (CHE-0234811). Finally, we thank Dr. Christopher Matranga (National Energy Technology Laboratory, US DOE), Dr. Alex V. Leontiev, Dr. Vaclav Stastny, and Albert Wong for valuable experimental advice.

[1] Self-assembling nanotubes: a) D. T. Bong, T. D. Clark, J. R. Granja, M. R. Ghadiri, *Angew. Chem.* **2001**, *113*, 1016–1041; *Angew. Chem. Int. Ed.* **2001**, *40*, 988–1011; b) S. J. Dalgarno, G. W. V. Cave, J. L. Atwood, *Angew. Chem.* **2006**, *118*, 584–588; *Angew. Chem. Int. Ed.* **2006**, *45*, 570–574; c) T. Yamaguchi, S. Tashiro, M. Tominaga, M. Kawano, T. Ozeki, M. Fujita, *J. Am. Chem. Soc.* **2004**, *126*, 10818–10819; d) S. Tashiro, M. Tominaga, T. Kusukawa, M. Kawano, S. Sakamoto, K. Yamaguchi, M. Fujita, *Angew. Chem.* **2003**, *115*, 3389–3392; *Angew. Chem. Int. Ed.* **2003**, *42*, 3267–3270; e) M. Tominaga, S. Tashiro, M. Aoyagi, M. Fujita, *Chem. Commun.* **2002**, 2038–2039; f) V. Sidorov, F. W. Kotch, G. Abdrakhmanova, R. Mizani, J. C. Fettinger, J. T. Davis, *J. Am. Chem. Soc.* **2002**, *124*, 2267–2278; g) L. Baldini, F. Sansone, A. Casnati, F. Ugozzoli, R. Ungaro, *J. Supramol. Chem.* **2002**, 219–226.

[2] Calixarene nanotubes: a) A. Ikeda, S. Shinkai, *J. Chem. Soc. Chem. Commun.* **1994**, 2375–2376; b) A. Ikeda, M. Kawaguchi, S. Shinkai, *An. Quim. Int. Ed.* **1997**, *93*, 408–414; c) S. K. Kim, W. Sim, J. Vicens, J. S. Kim, *Tetrahedron Lett.* **2003**, *44*, 805–809; d) S. K. Kim, J. Vicens, K.-M. Park, S. S. Lee, J. S. Kim, *Tetrahedron Lett.* **2003**, *44*, 993–997; e) S. K. Kim, J. K. Lee, S. H. Lee, M. S. Lim, S. W. Lee, W. Sim, J. S. Kim, *J. Org. Chem.* **2004**, *69*, 2877–2880; f) J.-A. Perez-Adelmar, H. Abraham, C. Sanchez, K. Rissanen, P. Prados, J. de Mendoza, *Angew. Chem.* **1996**, *108*, 1088–1090; *Angew. Chem. Int. Ed. Engl.* **1996**, *35*, 1009–1011; g) S. Le Gac, X. Zeng, O. Reinaud, I. Jabin, *J. Org. Chem.* **2005**, *70*, 1204–1210; other covalently linked nanotubes: h) A. Harada, J. Li, M. Kamachi, *Nature* **1993**, *364*, 516–518; this was the first covalently linked synthetic nanotube; the tubular polymer was prepared by cross-linking of polyrotaxane-threaded α-cyclodextrins; i) Y. Kim, M. F. Mayer, S. C. Zimmerman, *Angew. Chem.* **2003**, *115*, 1153–1158; *Angew. Chem. Int. Ed.* **2003**, *42*, 1121–1126; j) T. Iwanaga, R. Nakamoto, M. Yasutake, H. Takemura, K. Sako, T. Shinmyozu, *Angew. Chem.* **2006**, *118*, 3725–3729; *Angew. Chem. Int. Ed.* **2006**, *45*, 3643–3647.

[3] For timely overviews on synthesis and applications of calixarenes, see: a) *Calixarene 2001* (Eds.: Z. Asfari, V. Böhmer, J. Harrowfield, J. Vicens), Kluwer Academic, Dordrecht, **2001**; b) *Calixarenes in the Nanoworld* (Eds.: J. Vicens, J. Harrowfield) Springer, Dordrecht, **2006**.

[4] a) D. J. Cram, J. M. Cram, *Container Molecules and their Guests*, Royal Society of Chemistry, Cambridge, **1994**; cavitands: b) D. M. Rudkevich, J. Rebek, Jr., *Eur. J. Org. Chem.*, **1999**, 1991–2005; c) B. W. Purse, J. Rebek, Jr., *Proc. Natnl. Acad. Sci. USA* **2005**, *102*, 10777–10782; carcerands and hemicarcerands: d) A. Jasat, J. C. Sherman, *Chem. Rev.* **1999**, *99*, 931–967; e) R. Warmuth, J. Yoon, *Acc. Chem. Res.* **2001**, *34*, 95–105; f) R. Warmuth, *Eur. J. Org. Chem.* **2001**, 423–437; cryptophanes: g) A. Collet, J.-P. Dutasta, B. Lozach, J. Canceill, *Top. Curr. Chem.* **1993**, *165*, 103–129. Self-as-

sembling capsules: h) J. de Mendoza, *Chem. Eur. J.* **1998**, *4*, 1373–1377; i) F. Hof, S. L. Craig, C. Nuckolls, J. Rebek, Jr., *Angew. Chem.* **2002**, *114*, 1556–1578; *Angew. Chem. Int. Ed.* **2002**, *41*, 1488–1508; j) J. Rebek, Jr., *Chem. Commun.* **2000**, 637–643; k) D. M. Rudkevich in *Calixarene 2001* (Eds.: Z. Asfari, V. Böhmer, J. Harrowfield, J. Vicens), Kluwer Academic, Dordrecht, **2001**, p. 155–180; l) M. Fujita, K. Umemoto, M. Yoshizawa, N. Fujita, T. Kusukawa, K. Biradha, *Chem. Commun.* **2001**, 509–518; m) D. M. Rudkevich in *Functional Artificial Receptors* (Eds.: T. Shrader, A. D. Hamilton, Wiley-VCH, **2005**, pp. 257–298.

[5] a) N. Sakai, J. Mareda, S. Matile, *Acc. Chem. Res.* **2005**, *38*, 79–87; b) S. Matile, A. Som, N. Sorde, *Tetrahedron* **2004**, *60*, 6405–6435; c) S. Matile, *Chem. Soc. Rev.* **2001**, *30*, 158–167.

[6] a) A. N. Khlobystov, D. A. Britz, G. A. Briggs, *Acc. Chem. Res.* **2005**, *38*, 901–909; b) M. Monthioux, *Carbon* **2002**, *40*, 1809–1823; c) O. Vostrowsky, A. Hirsch, *Angew. Chem.* **2004**, *116*, 2380–2383; *Angew. Chem. Int. Ed.* **2004**, *43*, 2326–2329.

[7] For our preliminary communications on shorter synthetic tubes, see a) V. G. Organo, A. V. Leontiev, V. Sgarlata, H. V. R. Dias, D. M. Rudkevich, *Angew. Chem.* **2005**, *117*, 3103–3107; *Angew. Chem. Int. Ed.* **2005**, *44*, 3043–3047; b) G. V. Zyryanov, D. M. Rudkevich, *J. Am. Chem. Soc.* **2004**, *126*, 4264–4270.

[8] Molecular encapsulation of gases: a) D. M. Rudkevich, A. V. Leontiev, *Aust. J. Chem.* **2004**, *57*, 713–722; b) D. M. Rudkevich, *Angew. Chem.* **2004**, *116*, 568–581; *Angew. Chem. Int. Ed.* **2004**, *43*, 558–571.

[9] R. Rathore, S. V. Lindeman, K. S. S. Rao, D. Sun, J. K. Kochi, *Angew. Chem.* **2000**, *112*, 2207–2211; *Angew. Chem. Int. Ed.* **2000**, *39*, 2123–2127.

[10] a) G. V. Zyryanov, Y. Kang, D. M. Rudkevich, *J. Am. Chem. Soc.* **2003**, *125*, 2997–3007; b) Y. Kang, D. M. Rudkevich, *Tetrahedron* **2004**, *60*, 11219–11225; experiments with wider and more flexible *O*-peralkylated calix[5]-, calix[6]-, and calix[8]arenes did not lead to NO^+ entrapment. No characteristic color change was detected upon mixing with NO_2/N_2O_4.

[11] S. Kim, J. S. Kim, S. K. Kim, I.-H. Suh, S. O. Kang, J. Ko, *Inorg. Chem.* **2005**, *44*, 1846–1851.

[12] J. S. Kim, O. J. Shon, J. W. Ko, M. H. Cho, I. Y. Yu, J. Vicens, *J. Org. Chem.* **2000**, *65*, 2386–2392.

[13] a) R. Begum, T. Sagawa, S. Masatoki, H. Matsuura, *J. Mol. Struct.* **1998**, *442*, 243–250; b) A. L. Hofacker, J. R. Parquette, *Angew. Chem.* **2005**, *117*, 1077–1081; *Angew. Chem. Int. Ed.* **2005**, *44*, 1053–1057.

[14] This was confirmed by NOESY for the nitrosonium-filled nonsymmetrical, *O*,*O*′-dimethylated derivative of **7**.

[15] At this stage, the location of nitrate counterions in complexes **1**·$(NO^+)_2$–**4**·$(NO^+)_5$ has not been determined experimentally. Obtaining single crystals for X-ray analysis has proved difficult, as calixarene–nitrosonium complexes tend to decompose upon prolonged standing. Molecular modeling strongly suggests that these anions, which are too bulky to enter the tube interior, stay outside, in rather close proximity to the exterior in apolar solvent.

[16] V. Sgarlata, V. G. Organo, D. M. Rudkevich, *Chem. Commun.* **2005**, 5630–5632.

[17] a) E. Iglesias, J. Casado, *Int. Rev. Phys. Chem.* **2002**, *21*, 37–74; b) P. G. Wang, M. Xian, X. Tang, X. Wu, Z. Wen, T. Cai, A. J. Janczuk, *Chem. Rev.* **2002**, *102*, 1091–1134.

[18] E. Bosch, J. K. Kochi, *J. Org. Chem.* **1994**, *59*, 3314–3325.

[19] A somewhat similar effect was described elsewhere: N. Chopra, C. Naumann, J. C. Sherman, *Angew. Chem.* **2000**, *112*, 200–202; *Angew. Chem. Int. Ed.* **2000**, *39*, 194–196.

[20] For allosteric effects in supramolecular chemistry, see a) M. Takeuchi, M. Ikeda, A. Sugasaki, S. Shinkai, *Acc. Chem. Res.* **2001**, *34*, 865–873; b) S. Shinkai, M. Ikeda, A. Sugasaki, M. Takeuchi, *Acc. Chem. Res.* **2001**, *34*, 494–503.

[21] a) E. K. Kim, J. K. Kochi, *J. Am. Chem. Soc.* **1991**, *113*, 4962–4974; b) D. B. Keck, C. D. Hause, *J. Mol. Spectrosc.* **1968**, *26*, 163–174; for spectroscopic properties of arene–nitrosonium complexes, see G. I. Borodkin, V. G. Shubin, *Russ. Chem. Rev.* **2001**, *70*, 211–230.

[22] a) G. S. Heo, P. E. Hillman, R. A. Bartsch, *J. Heterocycl. Chem.* **1982**, *19*, 1099–1103; b) S. Ricard, P. Audet, R. Savoie, *J. Mol. Struct.* **1988**, *178*, 135–140; c) K. Y. Lee, D. J. Kuchynka, J. K. Kochi, *Inorg. Chem.* **1990**, *29*, 4196–4204.

[23] a) S. G. Bott, H. Prinz, A. Alvanipour, J. L. Atwood, *J. Coord. Chem.* **1987**, *16*, 303–309; b) U. Russo, A. Cassol, A. Silvestri, *J. Organomet. Chem.* **1984**, *260*, 69–72.

[24] For a detailed discussion of oscillation of a single metal cation in nanotubes, see reference [2b]. Two possible scenarios were proposed: intracalixarene metal tunneling and intercalixarene metal hopping.

[25] Preliminary experiments with Li^+Pic^- and Na^+Pic^- in $(CDCl_2)_2$ resulted in no complexation with the nanotubes.

[26] The U.S. EPA site on NO_x gases: http://www.epa.gov/air/urbanair/nox/index.html

[27] Y. Kang, G. V. Zyryanov, D. M. Rudkevich, *Chem. Eur. J.* **2005**, *11*, 1924–1932.

[28] For reviews on nitric oxide, see a) S. Pfeiffer, B. Mayer, B. Hemmens, *Angew. Chem.* **1999**, *111*, 1824–1844; *Angew. Chem. Int. Ed.* **1999**, *38*, 1714–1731; b) A. R. Butler, D. L. H. Williams, *Chem. Soc. Rev.* **1993**, 233–241.

[29] Simultaneous encapsulation: J. Rebek, Jr., *Angew. Chem.* **2005**, *117*, 2104–2115; *Angew. Chem. Int. Ed.* **2005**, *44*, 2068–2078.

[30] Nanoscale molecular containers: D. M. Rudkevich, *Bull. Chem. Soc. Jpn.* **2002**, *75*, 393–413.

[31] a) C. D. Gutsche, M. Iqbal, *Org. Synth.* **1990**, *68*, 234–237; b) C. D. Gutsche, J. A. Levine, P. K. Sujeeth, *J. Org. Chem.* **1985**, *50*, 5802–5806.

[32] W. Verboom, S. Datta, Z. Asfari, S. Harkema, D. N. Reinhoudt, *J. Org. Chem.* **1992**, *57*, 5394–5398.

[33] MacroModel 7.1; MM2 and Amber* Force Field. See: F. Mohamadi, N. G. Richards, W. C. Guida, R. Liskamp, M. Lipton, C. Caufield, G. Chang, T. Hendrickson, W. C. Still, *J. Comput. Chem.* **1990**, *11*, 440–467.

Received: October 29, 2006
Revised: December 12, 2006
Published online: February 13, 2007

